

## Article

# Multi-Objective-Based Charging and Discharging Coordination of Plug-in Electric Vehicle Integrating Capacitor and OLTC

Junaid Bin Fakhru Islam <sup>1,2</sup>, Mir Toufikur Rahman <sup>3</sup>, Shameem Ahmad <sup>1,4,\*</sup>, Tofael Ahmed <sup>5</sup>,  
G. M. Shafiullah <sup>6,\*</sup>, Hazlie Mokhlis <sup>1</sup>, Mohamadariiff Othman <sup>1</sup>, Tengku Faiz Tengku Mohmed Noor Izam <sup>1</sup>,  
Hasmainsi Mohamad <sup>7</sup> and Mohammad Taufiqul Arif <sup>8</sup>

<sup>1</sup> Department of Electrical Engineering, Universiti Malaya, Kuala Lumpur 50603, Malaysia

<sup>2</sup> Department of Electrical Engineering, Sheikh Fazilatunnesa Mujib University, Jamalpur 2000, Bangladesh

<sup>3</sup> School of Engineering, RMIT University, Melbourne 3000, Australia

<sup>4</sup> Department of Electrical and Electronic Engineering, Faculty of Engineering, American International University-Bangladesh (AIUB), Dhaka 1229, Bangladesh

<sup>5</sup> Department of Electrical and Electronic Engineering, Chittagong University of Engineering & Technology, Chittagong 4349, Bangladesh

<sup>6</sup> Discipline of Engineering and Energy, Murdoch University, Perth 6150, Australia

<sup>7</sup> Department of Electrical Engineering, University of Technology Mara (UiTM), Shah Alam 40450, Malaysia

<sup>8</sup> School of Engineering, Deakin University, Waurn Ponds, Geelong 3216, Australia

\* Correspondence: ahmad.shameem@aiub.edu (S.A.); gm.shafiullah@murdoch.edu.au (G.M.S.)

**Abstract:** The integration of plug-in electric vehicles (PEVs) in residential distribution networks demands a significant amount of electrical load where random and uncoordinated charging affects the quality and performance of the distribution network. Random and uncoordinated charging may increase the peak demand and can increase stress on critical network assets such as line, transformer, and switching devices. Moreover, the charging of PEVs in a low network reduces the voltage of the system below the lower limit. On the other hand, using PEVs as storage in the V2G mode can improve the network condition. Therefore, it is critical to properly manage the charging and discharging operation of PEVs. This paper proposes a multi-objective-based charging and discharging coordination of PEVs with the operation of the capacitor and on-load tap changer (OLTC). With the proposed strategy, the distribution network is operated safely, and charging is ensured for all PEVs connected to the network. The main consideration of this research is to reduce the daily power loss, operational cost, and voltage deviation of the system. The metaheuristic optimization binary firefly algorithm (BFA) has been applied to coordinate PEV charging and discharging as well as capacitor and OLTC operation in the system. A modified IEEE 31 bus 23 kV distribution system is used to implement the proposed strategy. From the obtained results, it is found that the combined PEV charging and discharging coordination with capacitor and OLTC operation reduces the power loss and cost by 34.16% and 12.68%, respectively, with respect to uncoordinated charging and enhances the voltage condition of the network.

**Keywords:** charging coordination; cost minimization; discharging coordination; plug-in electric vehicle



**Citation:** Islam, J.B.F.; Rahman, M.T.; Ahmad, S.; Ahmed, T.; Shafiullah, G.M.; Mokhlis, H.; Othman, M.; Izam, T.F.T.M.N.; Mohamad, H.; Arif, M.T. Multi-Objective-Based Charging and Discharging Coordination of Plug-in Electric Vehicle Integrating Capacitor and OLTC. *Energies* **2023**, *16*, 2172. <https://doi.org/10.3390/en16052172>

Academic Editor: Byoung Kuk Lee

Received: 1 February 2023

Revised: 12 February 2023

Accepted: 17 February 2023

Published: 23 February 2023



**Copyright:** © 2023 by the authors. Licensee MDPI, Basel, Switzerland. This article is an open access article distributed under the terms and conditions of the Creative Commons Attribution (CC BY) license (<https://creativecommons.org/licenses/by/4.0/>).

## 1. Introduction

Plug-in electric vehicles have gained popularity as an alternative to internal combustion engine vehicles to assure clean and environment-friendly transportation. A survey study conducted by the International Energy Agency forecasted that there would be about 100 million PEVs worldwide by the year 2035 [1]. The mass integration of PEVs into the residential distribution network brings challenges to the electrical distribution network by creating additional load demand. There are several factors, including PEV charging time, charger capacity, charger location and PEV penetration [2], that can affect the distribution system performance. The random PEV charging strategy, which is widely known as uncoordinated charging, can cause distribution transformer overload, create enormous power

loss for a sudden period due to the excessive power demand of PEVs, lead to large voltage deviation, and increase the operational cost of the distribution network [3,4].

The influence of PEV charging on the distribution system can be minimized by coordinating the PEV charging activities, which is known as a coordinated smart charging infrastructure. In such effort, different metaheuristic techniques such as particle swarm optimization [5,6], firefly algorithm [7], artificial bee colony [8,9], harmony search algorithm [10], and genetic algorithm [11,12] are applied. In addition to that, during PEV charging coordination, different objectives such as minimization of distribution system power loss [13,14], voltage deviation [5,15], PEV charging cost and total operational cost of the distribution system [6,16], regulating the voltage and providing ancillary services have been achieved. Optimal charging time-based PEV charging coordination is proposed in [17]. Based on departure time, PEV charging is scheduled in such a way that lower tariff time PEV charging received priority. Through this strategy, power loss is reduced and PEV charging activities during the lower tariff time also reduce the charging cost. A workplace-based PEV charging coordination is developed in [11] for the employees. In this research, it has been found that for fast charging, the probability of integrating maximum PEVs is reduced with the strategy of reducing the daily total cost of the system. Moreover, it is seen that slow charging is feasible for integrating a maximum number of PEVs with the objective of reducing the peak to average ratio of power demand. An on-line hybrid fuzzy discrete particle swarm optimization is applied in coordinating PEV charging focusing on minimizing power loss and maximizing the delivered power supply to the PEV [13]. This strategy distribution system is capable of connecting the maximum number PEVs while maintaining the maximum power demand constant. The load management strategy with PEVs in a residential distribution network aimed at peak shaving and minimization of power loss with voltage regulation of the system, which is proposed in [14]. PEV charging will be coordinated in such a way that the power consumption curve of the system becomes flattened. A Time-of-Use (TOU) electricity tariff can be applied to lessen the cost of PEV charging along with the distribution system operational cost. In this method, PEV users are motivated to charge their vehicle in the off-peak hours. However, a large number of PEV charging during the off-peak period may overload the transformer if the activities of PEV charging are not properly managed. Considering this issue, a metaheuristic technique-based PEV coordination strategy is developed [6] for minimizing the cost of the distribution system using a TOU electricity tariff. In [15], a real-time smart load management using maximum sensitivity selection is proposed. This strategy reduces the daily power loss along with the generation cost of distribution system. A fuzzy-based PEV charging coordination is developed in [16] to reduce the total cost. The authors aimed to reduce the total cost of the system by minimizing the power loss of the system. Several research studies on optimization-based PEV charging techniques are proposed to coordinate PEV charging addressing the under-voltage scenario along with the peak power consumption [18–20]. Furthermore, in the low-voltage distribution network, the integration of PEV has had much impact on the voltage profile. To maintain the voltage constraints and improve the performance of the system, a variable charge-rate PEV charging method is proposed in [21]. However, the variable charge-rate may decrease the charging efficiency and require a longer time span. A switchable capacitor and OLTC operation in a distribution network can increase the voltage of the distribution network [22]. Following this strategy, the capacitor and OLTC operation is incorporated with a fixed rate PEV charging coordination to enhance the voltage profile of the system during PEV charging coordination [5]. A specific PEV charging period is considered for optimal PEV charging coordination in [23]. In this method, distribution generators provide the extra power which is required for PEVs after utilizing the maximum power demand constraints. Moreover, distribution generators also enhance the voltage profile and reduce the power loss of the distribution network.

Furthermore, PEVs can provide a unique vehicle-to-grid (V2G) service due to having storage capacities. When PEVs are connected to the distribution network, power can

be supplied to the grid [24] by discharging from PEV batteries. The conception of the V2G application may expand the performance of a distribution network regarding system efficiency, generation dispatch, reliability and stability [25,26]. An energy resources management strategy with PEV integration is proposed in [27]. Based on the electricity price, charging–discharging cost is calculated to find an economical operation of the system providing reserve capacity by PEVs. An event-triggered scheduling strategy for V2G operation is conducted to reduce the overall load variance in a smart grid [28]. To ensure the power transmission safety of branches, an optimization model of PEV charging and discharging is proposed in [29]. Moreover, this model also reduces load fluctuations and maximizes the PEV owner's benefit. In order to optimally transfer power between PEV and the grid, the authors [30] recommended a multi-objective genetic algorithm model with the objective of voltage regulation and load flattening. Furthermore, an adaptive neuro-fuzzy inference system is implemented to maximize the use of storage from PEV batteries and minimize charging cost. Two PEV charging strategies with the objective of load curve shaping are proposed in [31] where a PEV charging and discharging coordination method are found to be more effective than only the charging method. A parking lot-based PEV charging and discharging coordination of PEV is studied in [32]. Different time periods are considered for the charging and discharging of PEVs such as charging when the energy cost is lower and discharging when the energy cost is higher. Through this strategy, the profit of the parking lot is increased.

Most of the researchers have studied only the PEV charging coordination in the distribution network. However, with the development of technology, the V2G strategy allows PEV batteries to send back power to the grid, and the application of V2G helps to build a set of instantly available distributed storage devices [24,25,27–32]. In addition, to improve the mileage of PEV, a higher capacity battery is starting to be used, and for that, a higher capacity charger (6.6 kW and 7.2 kW) is starting to be utilized, which is only considered in [5,6,13,21]. In the peak hours, PEV discharging operation in a residential distribution network can be provided by the V2G strategy. At the same time, the integration of a higher capacity PEV charger imposes a negative impact, such as increasing power loss due to high power demand and decreasing the voltage of the network during the PEV charging activities. Moreover, the coordination of PEV with multi-objective functions such as reducing the power loss, total cost and voltage deviation of a system is not covered previously in the literature. Thus, the multi-objective coordination of PEV charging and discharging with a variety of charger capacity in a residential distribution network is imperative to analyze the impact of integrating various capacity PEV chargers. In addition, there is no research available in the literature regarding PEV charging and discharging coordination that utilizes capacitor and OLTC operation to maintain the voltage constraints at the end buses. Considering the boundaries of the previous work, this paper proposes a multi-objective charging and discharging coordination of PEV in a residential distribution network integrating capacitor and OLTC operation.

The contributions of the paper are summarized as follows:

- (i) Multi-objective PEV charging and discharging coordination is developed minimizing power loss, voltage deviation and the total cost of the distribution system.
- (ii) According to the departure time, we propose a strategy that provides PEV charging with lower cost.
- (iii) Integrating capacitor and OLTC operation with charging and discharging coordination of PEVs to ensure charging for all PEV users in the distribution network.

The rest of the paper is organized as follows: the mathematical formulation of the developed charging and discharging coordination and system constraints is presented in Section 2. The methodology of the proposed study is described in Section 3, where the BFA optimization technique and AHP method for weighting factor determination are described. In Section 4, the computational procedure of BFA implementation in developing PEV charging and discharging coordination with capacitor and OLTC coordination has been described. Then, Section 5 contains the test system and modeling of PEV for the system.

Simulation results for different case studies are presented in Section 6. In the same section, statistical analysis of different case studies and comparison of the proposed study with other studies are presented. Lastly, Section 7 contained the conclusion of this paper.

## 2. Problem Formulation

In this paper, the main objectives are to minimize the power loss, total daily operational cost, and voltage deviation of the system. The total daily operational cost is minimized by minimizing power loss and charging PEVs at a lower tariff period. Capacitor switching and OLTC adjustment are employed in order to enhance the voltage profile of the system. To obtain a near-real-time scenario, simulation is performed with 5 min intervals. Thus, there are a total of 288 timeslots in one day.

### 2.1. Objective Function

The fitness function of the multi-objective optimization procedure can be formulated as:

$$F = \min(w_1 \times P_{loss} + w_2 \times TC + w_3 \times \Delta V) \quad (1)$$

where  $P_{loss}$  is the total power loss of the system,  $TC$  is the total daily operational cost of the system and  $\Delta V$  is the voltage deviation. In multi-objective optimization,  $w_1, w_2, w_3$  are the weighting factor for three considered objective functions, respectively. The objective functions are mathematically formulated as follows:

Objective function 1 (OF1): The total power loss of the system is represented by-

$$P_{loss} = \sum_{i=1}^{\text{timeslot}} (I_{b,i}^2 \times R_b) \quad (2)$$

Here,  $I_{b,i}$  is the current of branch  $b$  at timeslot  $i$  and the resistance of the branch is  $R_b$ .

Objective function 2 (OF2): The total cost of the system is the daily operational cost of the system, and it is determined by summation of the cost of total energy consumption with the cost of power loss in every timeslot that can be expressed as

$$TC = \sum_{i=1}^{288} ((P_{RSD} \times T_R) + (P_{PEV} \times T_{PEV}) + (P_{loss} \times T_{loss})) \quad (3)$$

$P_{RSD}$  is the residential power demand, and  $P_{PEV}$  is the PEV charging and discharging power. The cost of PEV is positive during charging, while in the case of discharging, the cost is negative.  $T_R$  is the tariff for residential load,  $T_{PEV}$  is the charging and discharging tariff, and  $T_{loss}$  is the tariff for power loss. For a single PEV, the charging and discharging power can be found by Equations (4) and (5).

$$P_{PEV}^{ch} = CHG_k \times (SOC_{req} - SOC_t) \times \frac{1}{\text{Charger Efficiency}} \quad (4)$$

$$P_{PEV}^{dch} = CHG_k \times (SOC_t - SOC_{min}) \times \frac{1}{\text{Charger Efficiency}} \quad (5)$$

where the  $k$ th PEVs charger capacity is  $CHG_k$ .  $SOC_t$  is the state of charge (SOC) at time  $t$ ,  $SOC_{min}$  is the minimum and  $SOC_{req}$  is the demanded SOC for a PEV, respectively.

Objective function 3 (OF3): The difference between the rated voltage and real voltage is termed as voltage deviation, which is denoted by

$$\Delta V = \text{Max}_{i=2}^m \left( \frac{V_{rated} - V_i}{V_i} \right) \quad (6)$$

The rated voltage  $V_{rated}$  for this system is considered as 1.0 p.u., and the real-time voltage at the  $i$ th node is  $V_i$ . There are  $m$  numbers of nodes in the system.

### 2.2. System Constraints

(a) Power balance and maximum demand

$$P_G(t) \geq (P_{RSD} + P_{PEV})_t \tag{7}$$

$P_G$  is the power consumption from the grid.  $P_{PEV}$  is positive at the time of charging and negative at the time of discharge.

(b) Bus voltage: To assure the quality of power and secure operation of the distribution network, the allowable maximum and minimum voltages are defined as:

$$V_{min} \leq V_b \leq V_{max} \tag{8}$$

$V_b$  is the bus voltage at time  $t$ .  $V_{min}$  and  $V_{max}$  are the lowest and highest acceptable voltage limit. In this research, maximum voltage deviation is considered 0.1 p.u.

(c) State of charge (SOC): The fractional amount of energy remaining in a PEV battery is regarded as the state of charge of the respective PEV battery.

$$SOC_{min} < SOC_t < SOC_{max} \tag{9}$$

$SOC_t$  is the SOC of PEV at time  $t$ ,  $SOC_{min}$  is the minimum SOC during PEV discharging, and  $SOC_{max}$  is the full charge SOC demanded by the user.

(d) Number of capacitors switching in a day The capacitor in a secondary bus could be switched more than once. In this strategy, capacitor switching is coordinated hourly. The number of capacitors switching of one day can be expressed by

$$\sum_{h=1}^{24} C_{s,h} \oplus C_{s,h-1} \leq C_{sm} \tag{10}$$

where the capacitor status at hour  $h$  is  $C_{(s,h)}$ .  $C_{sm}$  is the maximum capacitor switching in a day.

(e) OLTC switching in a day: The maximum number of switching can be given by,

$$\sum_{h=1}^{24} Tap_h - Tap_{h-1} \leq K_t \tag{11}$$

where  $Tap_h$  is the tap position for hour  $h$  and  $K_t$  is the highest acceptable number of OLTC switching for one day.

## 3. Methodology

The proposed research aims to develop an optimal PEV charging and discharging coordination using multi-objective metaheuristic optimization with the simultaneous coordination of capacitor switching and OLTC adjustment. In achieving the fitness function in Equation (1), the binary firefly algorithm (BFA) is used as an optimization technique to develop a near real-time (considering an interval of 5 min) PEV coordination in the distribution network. A time-of-use electricity tariff is used to minimize the total daily operational cost of the system. The proposed method is implemented in a residential distribution network provided with the smart grid facility with bi-directional power and communication architecture. The control and power flow with the communication architecture of the developed strategy is illustrated in Figure 1.

### 3.1. Optimization Framework

The firefly algorithm, inspired by the flashing behavior of fireflies, is a nature-inspired metaheuristic optimization technique proposed by Xin-She Yang in 2007 [33]. As well as particle swarm optimization, genetic algorithm, and evolutionary programming, the firefly algorithm (FA) is also a population-based metaheuristic optimization algorithm. On the other hand, FA differs from other optimization strategies in terms of modifying

the parameters with less dependency on the algorithm, and there is an accurately defined search space [7].

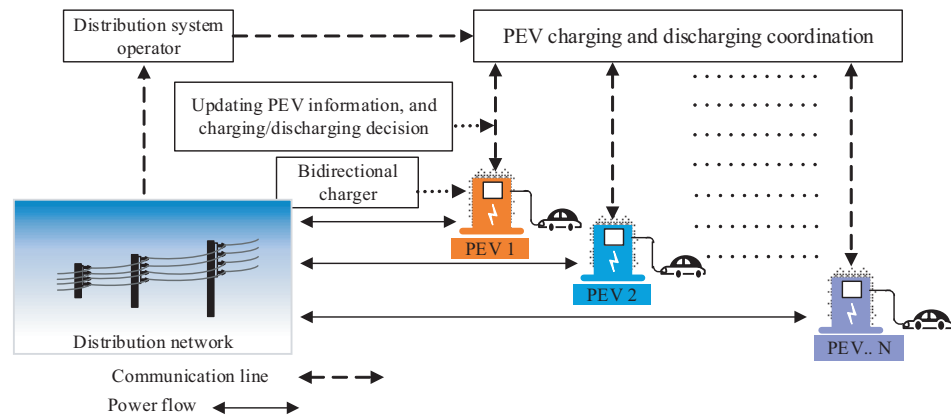


Figure 1. Schematic diagram of PEV coordination in a smart residential distribution system.

BFA is identical to the firefly algorithm, and the basic change is in the equation of changing the location of a firefly [34]. The following assumptions are considered during the implementation of the binary firefly algorithm.

- All the fireflies are regarded as the same gender and attract each other.
- The attractiveness between two fireflies is proportional to the brightness where brightness varies according to the distance between two fireflies. The objective function is used to calculate the brightness. Brighter fireflies are attracted by the bright fireflies.
- The fireflies will move randomly if any firefly with more brightness is not available. In the search space, the distance of two fireflies,  $i$ th and  $j$ th, can be calculated from the vector operation executed in Cartesian framework that can be expressed by

$$r_{ij} = \|Y_i - Y_j\| = \sqrt{\sum_{a=1}^d (Y_{id} - Y_{jd})^2} \quad (12)$$

Here,  $r$  is the distance between two fireflies. The dimension of the vector is  $S$ .  $Y_{i,d}$  and  $Y_{j,d}$  are the  $d$ th dimensions of  $Y_i$ ,  $Y_j$  fireflies, respectively.

The attraction between two fireflies is decreased when they moved in the opposite direction; thus, the separation between two fireflies is increased. The attraction between two fireflies can be described by:

$$\beta_r = \beta_0 \times \exp(-\gamma r^m); m \geq 1 \quad (13)$$

$\beta_{(r)}$  is the attractiveness at distance  $r$  and  $\beta_{(0)}$  is the attractiveness at  $r = 0$ .  $\gamma$  is the light absorption coefficient, and  $m$  represents the firefly's number, which is set as 2.

The bright firefly moves to the brighter firefly. The movement of a bright ( $j$ th) firefly to the brighter ( $i$ th) firefly can be represented by:

$$Y_i(t) = Y_i + \beta_0 \times \exp(-\gamma r^m); m \times \|Y_i - Y_j\| + V_j \quad (14)$$

$$V_j = \delta (rand - 0.05) \quad (15)$$

In Equation (14), the first term  $Y_j$  defines the instant position of the firefly  $j$ . The second term expresses the strength of brightness since  $j$ th firefly is attracted to the  $i$ th firefly.  $v_j$  is the end term that presents the movement of the  $j$ th firefly through the whole search space if it failed to find any fireflies with higher intensity. Moreover,  $\delta$  is a randomization parameter which is a fixed value within the scale of 0–0.5.

When the firefly  $j$  moves to firefly  $i$ , the position of firefly  $j$  is changed to a real number. Hence, it needs to change the real number to a binary number. The Sigmoid function is used to transfer the continuous number to a binary number.

$$S(Y_j) = \frac{1}{1+e^{-\gamma j}} \tag{16}$$

The changed position of firefly  $j$  is determined by the following piecewise relation.

$$Y_j(t) = \begin{cases} 1 & \phi < S(Y_j) \\ 0 & \phi > S(Y_j) \end{cases} \tag{17}$$

### 3.2. Analytic Hierarchy Process

Satty [35] has developed a systematic multi-criteria decision-making technique which is termed as analytic hierarchy process (AHP) and applied in different fields as well as power systems [36,37]. In this research, each objective function’s weighting factor is determined by employing AHP. The procedures of determining weighting factors using AHP are described as follows.

Considering each objective function as a criteria and setting the priority among the criteria, a pair-wise comparison matrix, which is termed as the criteria matrix  $PM_{criteria}$ , ( $n \times n$ ), is derived for the number of criteria  $n$  and presented in Equation (18).

$$[PM_{criteria}] = \begin{matrix} & \begin{matrix} Criteria_{n1} & Criteria_{n2} & Criteria_{n3} \end{matrix} \\ \begin{matrix} Criteria_{n1} \\ Criteria_{n2} \\ Criteria_{n3} \end{matrix} & \begin{bmatrix} 1 & \frac{Criteria_{n1}}{Criteria_{n2}} & \frac{Criteria_{n1}}{Criteria_{n3}} \\ \frac{Criteria_{n2}}{Criteria_{n1}} & 1 & \frac{Criteria_{n2}}{Criteria_{n3}} \\ \frac{Criteria_{n3}}{Criteria_{n1}} & \frac{Criteria_{n3}}{Criteria_{n2}} & 1 \end{bmatrix} \end{matrix} \begin{matrix} Criteria_{n1} \\ Criteria_{n2} \\ Criteria_{n3} \end{matrix} \tag{18}$$

The approximate method is applied to calculate the weights of each criterion because of its simplicity rather than the exact method. The normalization matrix  $NM_{criteria}$  is calculated from the criteria matrix using Equations (19) and (20).

$$criteria_{column} = [\sum column_1 \quad \sum column_2 \quad \sum column_3] \tag{19}$$

$$NM_{criteria} = \left[ \begin{matrix} \frac{(PM_{criteria})_i}{\sum column_1} & \frac{(PM_{criteria})_i}{\sum column_2} & \frac{(PM_{criteria})_i}{\sum column_3} \end{matrix} \right] \tag{20}$$

where the criteria numbers are indicated by  $i = 1, 2, 3$  row wise. Using the normalization matrix, the weighting factors ( $w_1, w_2, w_3$ ) are determined by calculating the average of every row employing the subsequent equation.

$$\begin{bmatrix} w_1 \\ w_2 \\ w_3 \end{bmatrix} = \begin{bmatrix} \frac{\sum (NM_{criteria})_j}{no. of criteria} \\ \frac{\sum (NM_{criteria})_j}{no. of criteria} \\ \frac{\sum (NM_{criteria})_j}{no. of criteria} \end{bmatrix} \tag{21}$$

where the criteria numbers are indicated by  $j = 1, 2, 3$  column wise. Determination of the consistency ratio (CR) of the pair-wise comparison matrix is obligatory when the weighting factors are calculated. The method of determining the CR is presented in [38]. To continue the AHP process, the value of CR must be 0.10 or less.

In this study, three criteria—power loss, operational cost and voltage deviation—are being considered. The AHP model of power loss, operational cost and voltage deviation for the proposed method and the criteria matrix is shown in Equation (22).

$$P_{loss} \quad Cost \quad dv$$

$$PM_{criteria} = \begin{bmatrix} 1 & 4 & 3 \\ \frac{1}{4} & 1 & 2 \\ \frac{1}{3} & \frac{1}{2} & 1 \end{bmatrix} \begin{matrix} P_{loss} \\ Cost \\ dv \end{matrix} \quad (22)$$

After solving Equation (22), the weighting factors are found as  $w_1 = 0.6196$ ,  $w_2 = 0.2243$  and  $w_3 = 0.1560$ . The consistency ratio (CR) of the proposed comparison matrix is 0.0942. It can be said that the pair-wise comparison matrix is free from inconsistency, since CR is smaller than 0.10. Consequently, the analysis of AHP of the proposed study is valid.

#### 4. Computational Procedure of the Proposed Method

The proposed computational procedure of PEV coordination, capacitor and OLTC adjustment is described in the following sections.

##### 4.1. Computational Procedure of PEV Charging and Discharging Coordination Using BFA

The following steps are:

- Step 1: All the required data, both distribution network and PEV, are taken as input. Optimization parameters are also set.
- Step 2: Fixed the timeslot at  $t = 1$  and create the initial population of fireflies in binary form for arrival of every PEV. Each firefly expresses the status of PEV chargers where "1" denotes that PEV connected to the system and "0" indicates that the charging or discharging of the corresponding PEV did not start or has already completed.
- Step 3: In every iteration, the power loss of the network and voltage level of every node is determined by executing backward forward load flow. The fitness function (Equation (1)) is evaluated.
- Step 4: According to the light intensity (fitness), the populations are ranked. Among them, the best value is determined.
- Step 5: Updating all the fireflies and rank the movement by considering the constraints using (12) to (17).
- Step 6: Repeat step 3 to step 5 until the maximum number of iterations is achieved.
- Step 7: Determine the best combination, and the charging–discharging decision of each PEV is sent to a residential charging station by using a smart bidirectional communication system.
- Step 8: The timeslot is updated, and disconnect the fully charged PEV/PEV discharged to a minimum level of SOC. In addition, consider those PEVs which did not connect in the previous timeslot and newly arrived PEVs at the present timeslot.

The flow chart of the charging and discharging coordination of PEV using the BFA is presented in Figure 2.

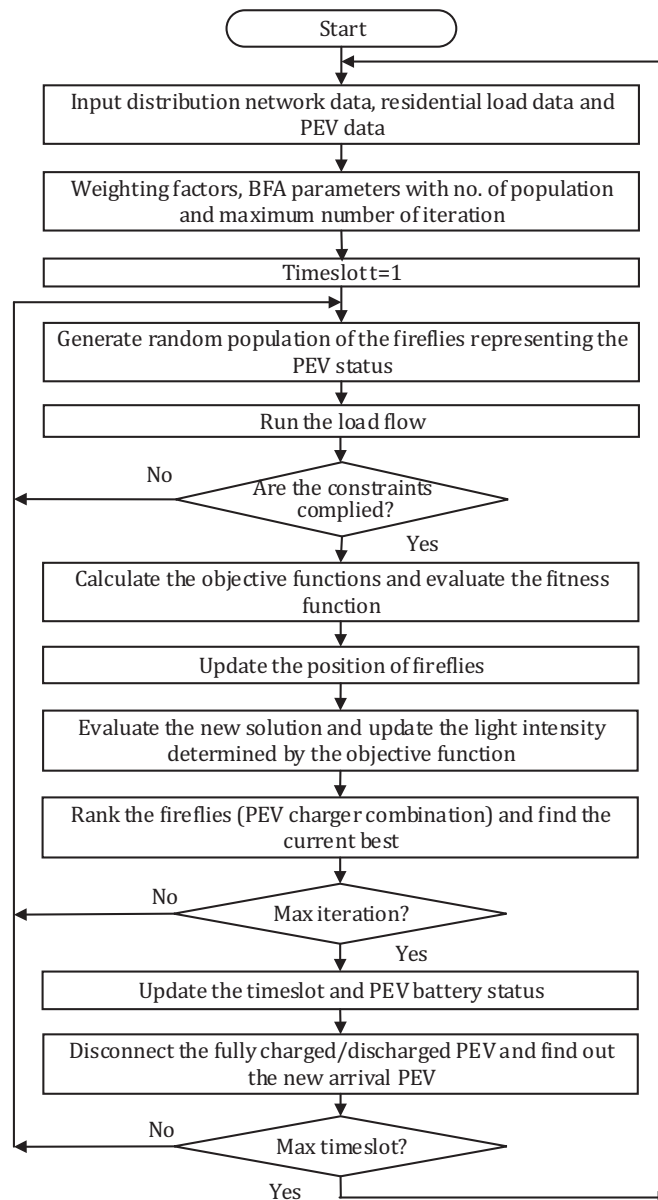


**Figure 2.** Flow chart of the PEV coordination with BFA algorithm.

#### 4.2. Computational Procedure of Capacitor Switching and OLTC Adjustment with BFA

The following steps are:

- Step 1: Input the network data, size and position of the capacitor in the network. Furthermore, the charger position with respective voltage is also taken.
- Step 2: Generate the initial population of the fireflies where each firefly describes the status of the capacitor. Each firefly as “1” expressed that a capacitor is in operation, and each firefly as “0” indicated that the capacitor is turned off.
- Step 3: Calculate the objective functions and fitness function.
- Step 4: According to the light intensity (fitness), the best value is determined and saved.
- Step 5: Update all the fireflies (change the switching combination) and rank the movement by considering the constraints using Equations (12)–(17).
- Step 6: The steps are repeated from step 3 until the maximum iteration.
- Step 7: Find out the best combination of the capacitor switching, and according to the voltage attained, the tap changer position is adjusted in accordance with 0.00625 voltage changes for each tap position.

The flow chart of the capacitor switching and OLTC adjustment using BFA is presented in Figure 3.

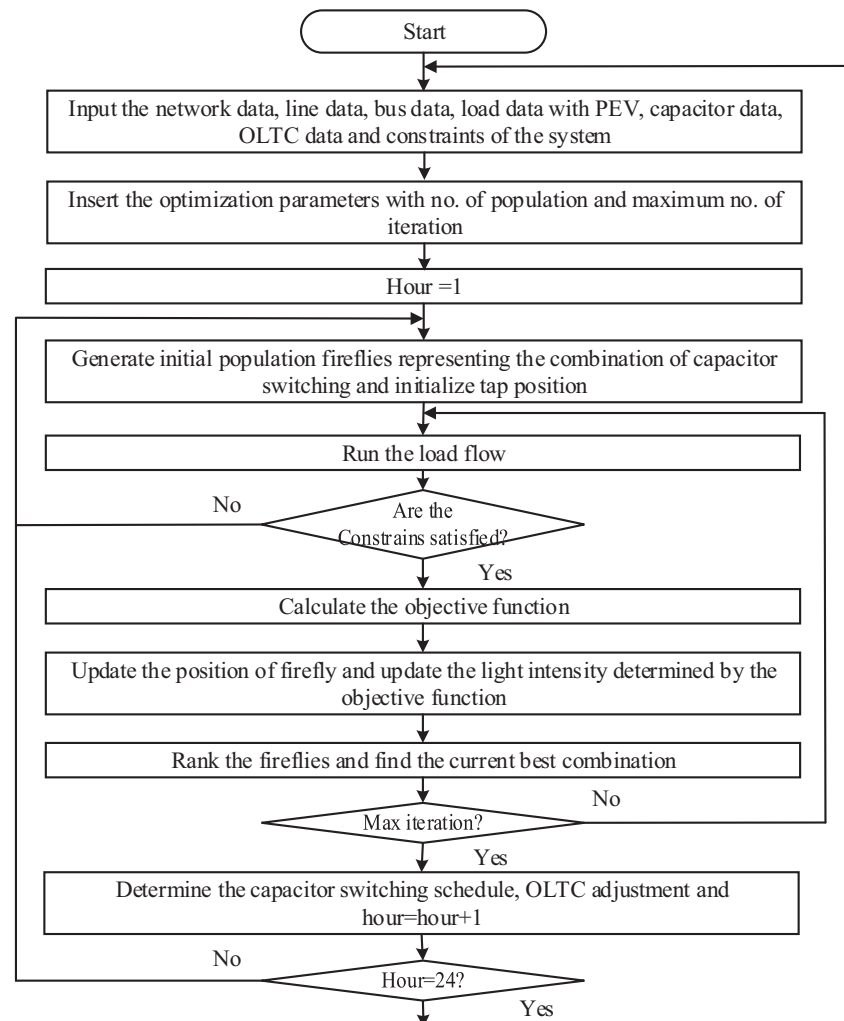


**Figure 3.** Flow chart of the capacitor switching and OLTC adjustment with PEV coordination.

It is considered that once a PEV is initiated for discharging, it will discharge up to 20% of the SOC. When a PEV has started to charge, it continues charging up to the requested level of SOC.

## 5. Test System Modeling

The test system, PEV penetration level, and PEV data with battery and charger capacity are described in this section.

### 5.1. System Architecture

A smart residential distribution network formed with the modified IEEE 31 bus 23 kV distribution system is used to implement the proposed strategy. Figure 4 presents the single line diagram of the distribution system containing 22 low-voltage feeders with 415 volts. Each feeder is connected with nineteen nodes, and each node is considered as a residential load. The number of total houses in the system is 418, and the maximum load in each house is 2 kW. PEV is randomly connected in the low-voltage feeder, and one house can have a maximum of one residential PEV charging station. The daily load profile and TOU electricity tariff is taken from [16] and illustrated in Figure 5. Five switchable capacitors are used in this system. The capacitors' location and corresponding capacity were taken from [5].

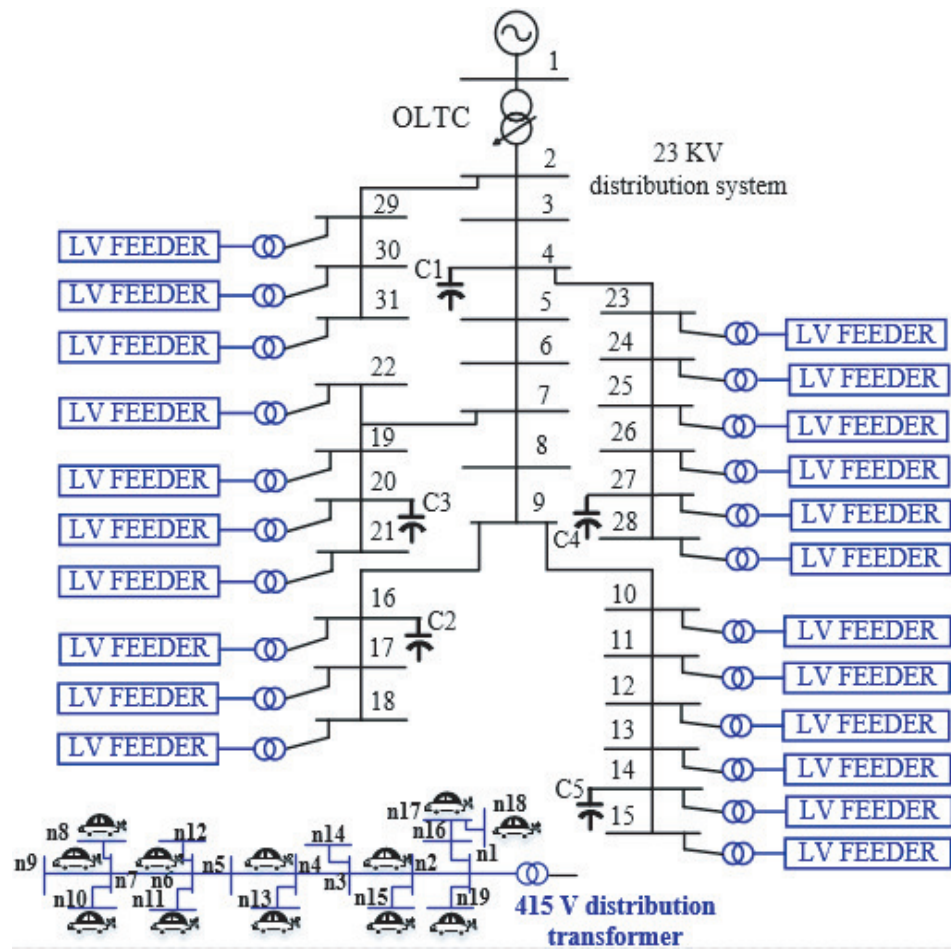


Figure 4. Modified IEEE 23kV 31 bus distribution network, and one feeder is populated with 63% PEV.

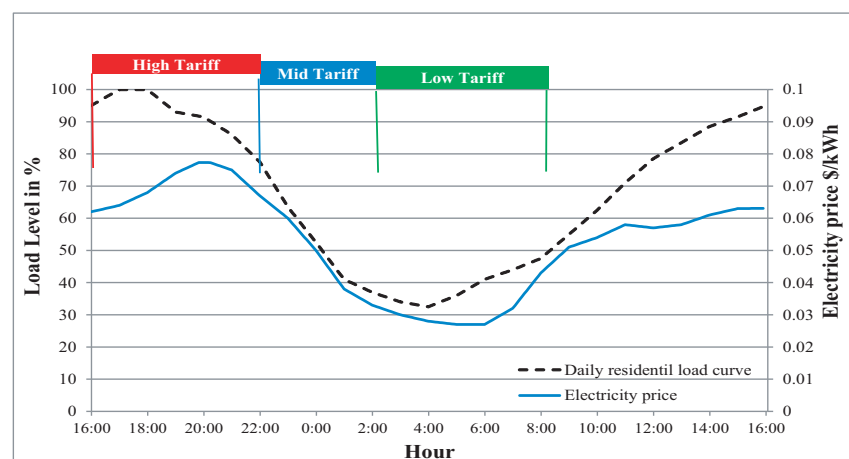


Figure 5. Daily load level and electricity price of the distribution system.

### 5.2. PEV Modeling

PEVs with three types of battery capacity, 10 kWh, 16.6 kWh and 19 kWh with charger capacities of 4 kW, 6.6 kW and 7.2 kW, respectively are chosen in this study. Three levels of PEV penetration (32%, 47% and 63%) are considered. Hence, in each feeder, there are 6, 9 and 12 PEVs and a total of 132, 198 and 264 PEVs in the system for 32%, 47% and 63% PEV penetration, respectively. In each penetration level, the 30% PEV is with a 4 kW charger and a 10 kWh battery, the 40% PEV is with a 6.6 kW charger and 16 kWh battery, and the 30% PEV is with a 7.2 kW charger and 19.2 kWh battery.

## 6. Result and Discussion

The numerical results of the case studies are described in this section. Before presenting the results of the coordinated charging and discharging strategy, the result of uncoordinated charging is described and taken as the reference case.

### 6.1. Case Studies

To observe the impact of PEV integration and find out the efficiency of the developed method, three case studies are studied as follows:

Case 1—Uncoordinated charging: In this method, PEV will start charging as soon as it plugs into the charging outlet.

Case 2—Coordinated charging and discharging: An optimization algorithm is applied to the coordinating charging and discharging operation of PEVs in the distribution system. Objective functions are considered and constraints are maintained in this case

Case 3—Coordinated charging and discharging with capacitor and OLTC. In this case, capacitor switching and OLTC adjustment is performed simultaneously with PEV charging and discharging operation. The necessity and benefit of capacitor switching and OLTC adjustment is described in detail in the Results section.

### 6.2. Case 1: Uncoordinated Charging

In this case, PEV starts to receive charge immediately after plugging into the charger, ignoring the system conditions. The uncoordinated charging creates higher active power demand in the system, which further causes enormous power loss with large voltage deviation. Figures 6–8 show the consequence of uncoordinated charging in terms of power consumption, power loss and voltage deviation of the distribution network, respectively. The maximum power consumption level of the system is 864 kW. From Figure 6, it is seen that for three levels of penetration, the PEV charging load along with the residential load has exceeded its maximum peak and overloaded the transformer. The power loss of the distribution network for three levels of PEV penetration is presented in Figure 7. The highest power loss for 63% PEV penetration is almost five times (at 18.00) compared to the power loss when the residential load is the highest. From Figure 8, it is found that the weakest node voltage (lowest voltage in the system) for 63% penetration is 0.6509 p.u at 18.00. Consequently, there is an undesirable increase in the total cost of the system. The increase in the total daily operational cost of the system is 19.85%, 29.50% and 37.52% for 32%, 47% and 63% PEV penetration compared to without PEVs in the system.

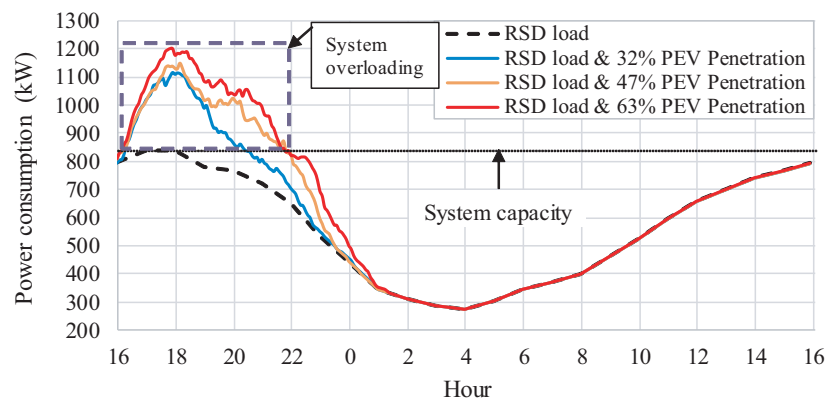
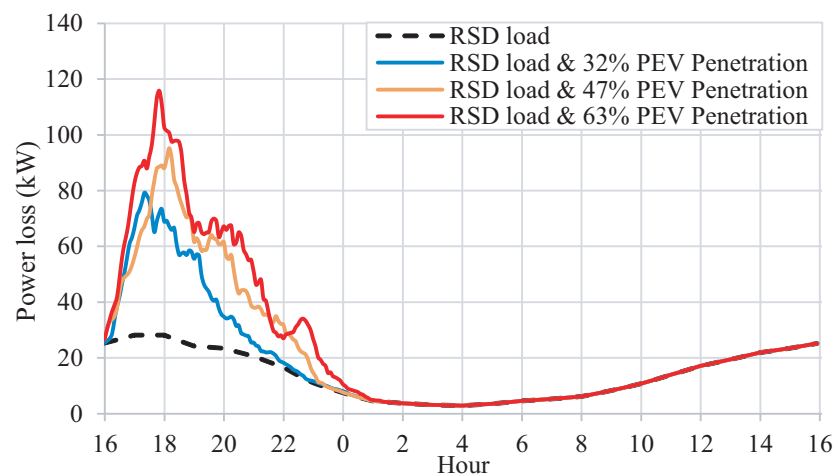
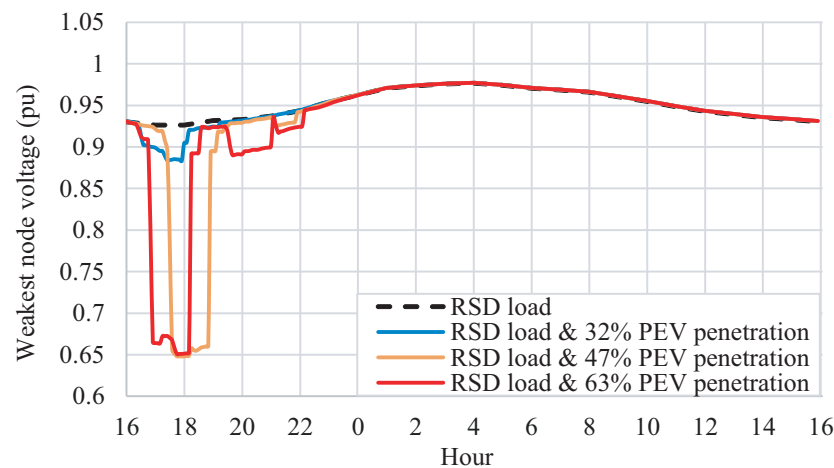


Figure 6. Distribution system power consumption in uncoordinated charging.



**Figure 7.** Power loss of the distribution system in uncoordinated charging.



**Figure 8.** Weakest node voltage profile of the system in uncoordinated charging.

### 6.3. Case 2: Coordinated Charging and Discharging

An approach considering a near real-time optimal charging and discharging coordination of PEV is presented in this case. Once at home, the PEV users plugged the vehicle in the charger located at their parking. However, PEVs will not start charging immediately. Based on the system constraints, an optimal charging or discharging coordination schedule will be allocated by the distribution system control unit, and after that, the decision will be sent to the bi-directional charging point, and accordingly, PEVs charging will be activated. The obtained results after applying the coordination technique are demonstrated in Figures 9–12. The total power consumption is shown in Figure 9. PEVs participate in V2G operation from the hours 4.00 p.m. to 10 p.m., which reduces the power consumption from the substation. The charging activities of PEV start from the early morning at 2.00 a.m., and power consumption is always within the maximum capacity of the system. Figure 10 shows the power loss of the system: for instance, for 63% PEV penetration, power loss is decreased by 36.39% in contrast to uncoordinated charging. Moreover, in this strategy, the voltage profile of the system is enhanced. As shown in Figure 11, the voltage of the weakest node is 0.90096 p.u., which is within the lower allowable limit. The system cost is reduced by 7.96%, 12.44% and 13.48% for 32%, 47% and 63% PEV, respectively, with respect to uncoordinated charging.

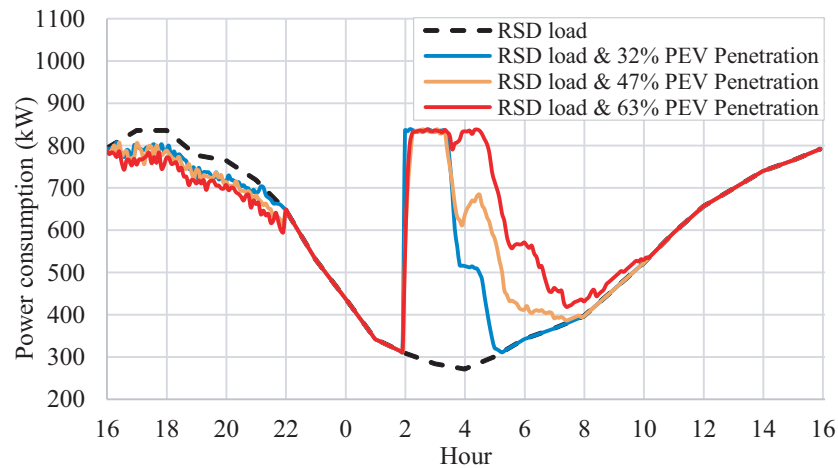


**Figure 9.** Distribution system power consumption in coordinated charging and discharging.

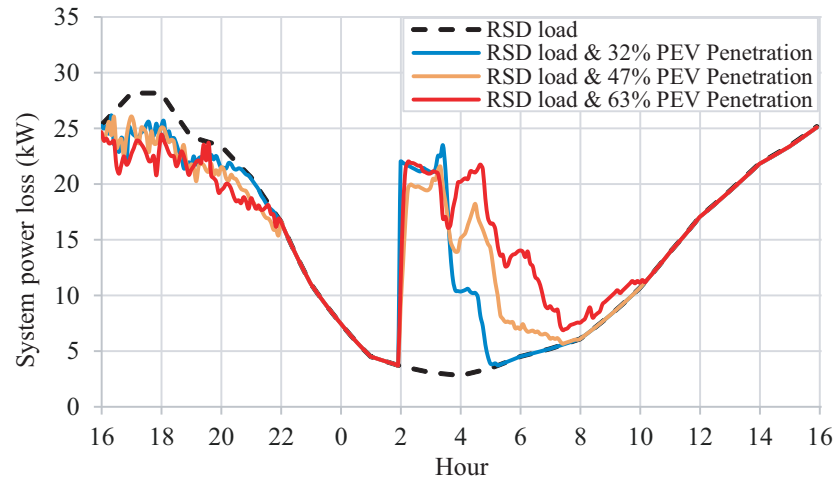


**Figure 10.** Power loss of the distribution system in coordinated charging and discharging.

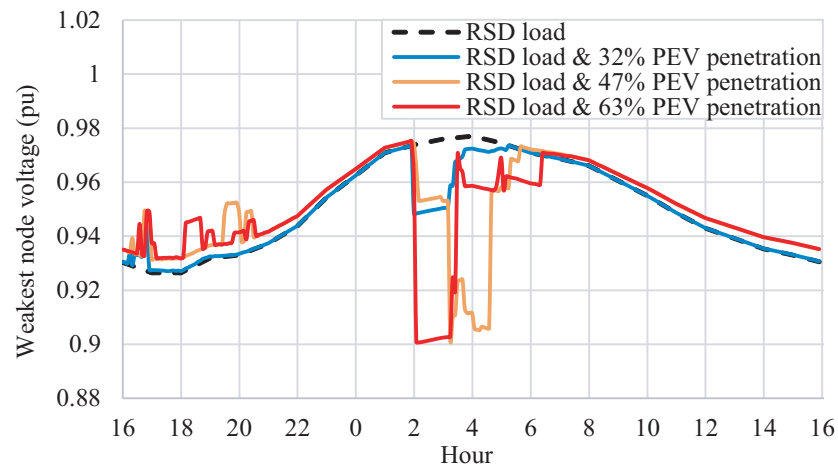


**Figure 11.** Weakest node voltage profile of the system in coordinated charging and discharging.

To check the charge level of PEV batteries, the SOC of PEVs can be analyzed. Figure 12 represents the SOC level of PEVs for the worst feeder (where lowest voltage have been found) of the system. From Figure 12, it is seen that after applying the coordination strategy, several PEVs still lack the requested level of SOC due to the voltage constraint. Basically, the voltage level at the end buses always remained close to the lower boundary, and if further loads (PEV charging) connect at this time, it violates the lower band of voltage. It

has been found that some PEVs in 16 feeders (a few PEVs in each feeder) did not receive charge according to the requested level of SOC. Since all the PEVs did not receive a full charge, this strategy failed to satisfy all the PEV users.

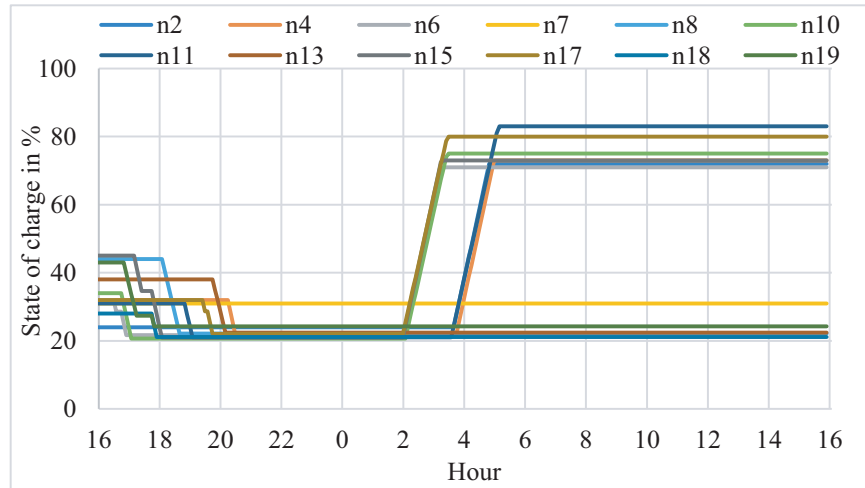


**Figure 12.** Weakest feeder PEV battery SOC of coordinated charging and discharging for 63% penetration.

6.4. Case 3: Coordinated Charging and Discharging with Capacitor and OLTC

To resolve the higher voltage deviation issue and to ensure the required charge for all PEVs, the switchable capacitor and OLTC operations are utilized simultaneously with the coordination of charging and discharging of PEVs. The key achievement of capacitor switching along with the adjustment of OLTC is to enhance and assure the voltage level of each node in the distribution network within the allowable range. The total power consumption is shown in Figure 13, and it is seen that the charging of PEVs is completed by the following morning, and there is no transformer overloading in the system. The power loss of the system is presented in Figure 14. Power loss is reduced by 34.16% with respect to Case 1 and slightly increased compared to Case 2, since all PEVs receive a full charge, whereas some PEVs did not connect in Case 2. The weakest node voltage profile of the system is shown in Figure 15. There are 6.08%, 6.63% and 7.03% voltage deviations for 32%, 47% and 63% PEV penetration, respectively. With respect to case study 1 and 2, the voltage profile is much improved in Case 3. The system cost is reduced by 8.08%, 11.70% and 12.68% for 32%, 47% and 63% PEV, respectively, compared to uncoordinated charging.

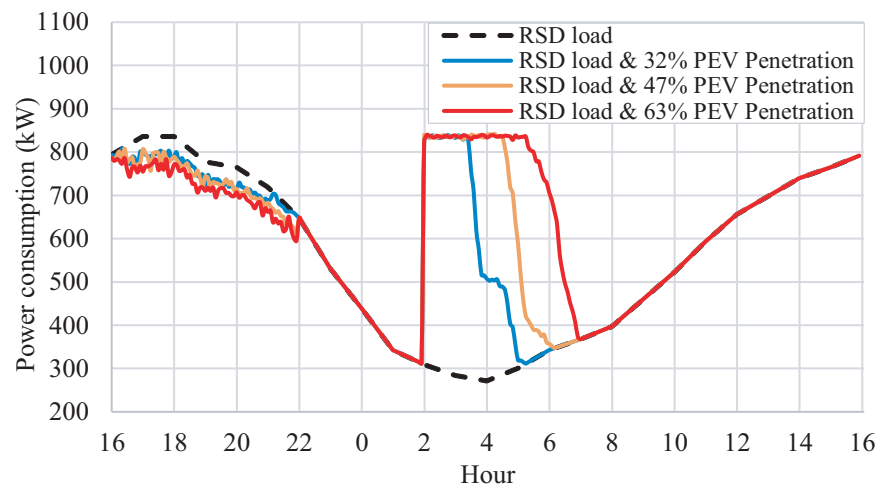


**Figure 13.** Distribution system power consumption in coordinated charging and discharging coordination with capacitor and OLTC.

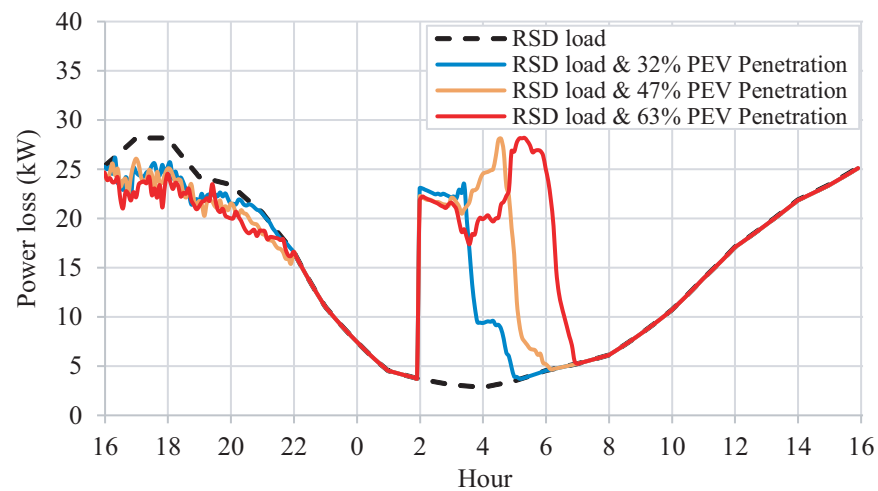


**Figure 14.** Power loss of the distribution system in coordinated charging and discharging with capacitor and OLTC.

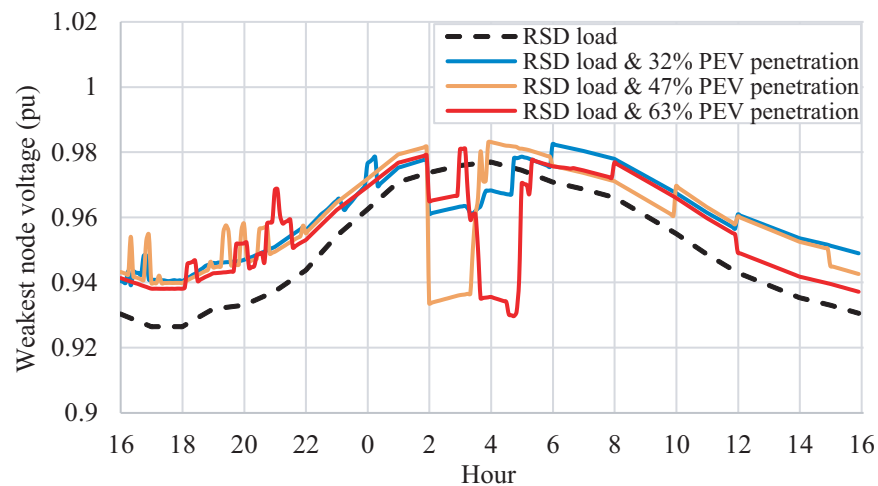


**Figure 15.** Weakest node voltage profile of the system in coordinated charging and discharging with capacitor and OLTC.

The SOC of PEVs of the weakest feeder is shown in Figure 16. After arriving at the residential charging point, PEVs participate in V2G operation at a high tariff time and start charging at a lower tariff time. It is seen from Figure 16 that all the PEVs of that feeder received full charge up to their requested level of SOC. No PEVs are left out in the system to receive charge, and customers are entirely satisfied.

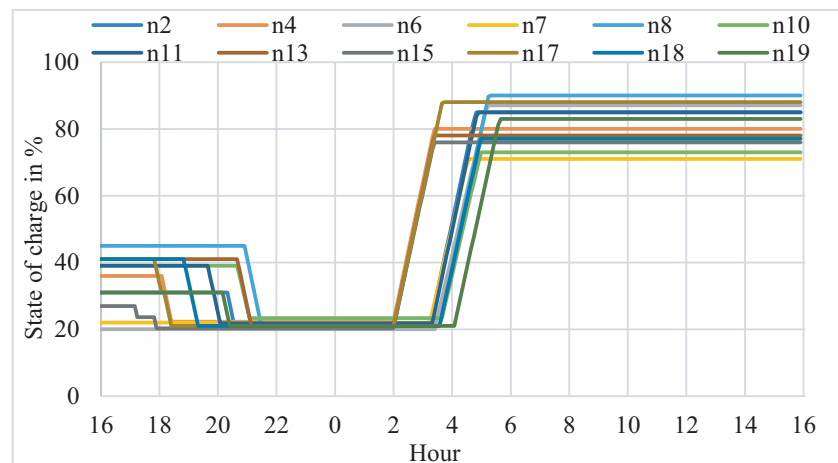


**Figure 16.** Weakest feeder PEV battery SOC of coordinated charging and discharging with capacitor and OLTC for 63% penetration.

### 6.5. Discussion and Comparison Studies

The overall comparison of the three case studies is presented in Table 1. In Case 1, power loss is excessively high and as well as large voltage deviation. There is a 39.41% increase in power loss and 35.19% increase in voltage deviation for the 63% PEV penetration compared to no PEVs in the system. Additional PEV power consumption and high-power loss in the peak hour increase the total operational cost of the system.

In Case 2, power loss is increased by 15.88%, which is much lower than uncoordinated charging. Voltage deviation is found within the allowable range. However, for 47% and 63% PEV penetration, a few PEVs in 16 feeders did not receive full charge due to the voltage constraints. Thus, the number of feeders where PEV received full charge is not satisfactory. In Case 2, the total cost is increased 18.98%, but it failed to ensure the full charge of all PEVs. In Case 3, power loss and cost are increased a little bit compared to Case 2 since a number of PEVs are newly connected in Case 3. The capacitor and OLTC operation in the distribution system significantly improved the voltage profile of the entire distribution network and ensured full charge for all PEVs.

**Table 1.** Quantitative comparison among case study 1, 2 and 3.

Case Study	PEV (%)	Increase in Power (%)	$\Delta V$ (%)	<sup>a</sup> Total Cost (\$)	<sup>b</sup> Increase in Total Cost (%)	<sup>c</sup> PEV Charge Complete Ratio
No PEV	-	-	7.36	786.20	-	-
Case 1	32	39.41	11.69	942.32	19.85	22/22
	47	61.84	35.19	1018.13	29.50	22/22
	63	85.18	34.90	1081.18	37.52	22/22
Case 2	32	8.34	7.29	867.25	10.31	22/22
	47	10.44	9.83	891.47	13.39	10/22
	63	15.88	9.93	935.42	15.88	6/22
Case 3	32	8.42	6.08	866.15	10.17	22/22
	47	14.37	6.63	898.94	14.34	22/22
	63	19.92	7.03	943.75	20.04	22/22

<sup>a</sup> increase in power loss with respect to no PEVs in the system; <sup>b</sup> increase in total cost with respect to no PEVs in the system; <sup>c</sup> number of feeders where the PEV received full charge/total number of feeders.

A comparison of the proposed study with other works in the literature is presented in Table 2. In comparison with the other researches, this paper developed a charging and discharging coordination of PEVs for a residential distribution network. In this research, a higher capacity PEV charger is considered both for PEV charging and discharging operation

where only the charging operation of PEV with a higher capacity charger is considered in [5,6,13,21]. Moreover, the proposed method is considered as a multi-objective function. After the discharging operation of the PEV, the capacitor and OLTC operation is integrated to ensure PEV charging throughout the entire distribution network.

**Table 2.** Comparison among different works in the literature.

Ref	Research Objective	PEV Coordination Type	Objective Function Type	Applied Method	Maximum Power Loss	Weakest Node Voltage	Customer Satisfaction Analysis
[5]	Minimizing power loss and voltage deviation	Charging coordination	Single	Binary PSO	29 kW	0.925 pu	Yes
[13]	Minimize cost, loss and maximize power delivery for PEV charging	Charging coordination	Single	Fuzzy discrete particle swarm optimization	32 kW	0.9 pu	No
[17]	Minimizing power loss	Charging coordination	Single	Binary evolutionary programming	33 kW	0.9 pu	No
[21]	Maximize customer satisfaction	Charging coordination	Single	Coordinated aggregated PSO	31 kW	0.9 pu	Yes
Proposed method	Minimizing power loss, operational cost and voltage deviation of the system	Charging and discharging coordination	Multi-objective	Binary firefly algorithm and analytic hierarchy method	28 kW	0.93 pu	Yes

## 7. Conclusions

A multi-objective PEV charging and discharging coordination is developed to lessen the impact of integration of PEVs on the distribution system. The key focus of this paper is to reduce the power loss, total daily operational cost, and voltage deviation of the system with PEV integration into the distribution system. It has been found that after applying a PEV coordination strategy, there is a significant improvement in the distribution system. With the developed coordinated PEV charging and discharging strategy, there is no transformer overloading, and the power loss and cost of the distribution system are reduced 34.16% and 12.68%, respectively, with respect to uncoordinated charging. The voltage profile of the system is enhanced where the lowest voltage level is 0.927 p.u., which results in decreasing voltage deviation. Through the discharging (V2G) operation of PEV, the power consumption from the distribution grid is reduced at the peak load period, and that also reduced the cost of the system. Capacitor and OLTC adjustment enhance the voltage profile of the system and ensure the full charge of all PEVs in the network. The application of a TOU electricity tariff minimized the total operational cost of the system. Moreover, PEV users will be inspired to participate in V2G operation, since the proposed strategy is ensured, obtaining the full charge of all PEVs before leaving the next morning. For the future study, PEV coordination can be developed with combined operation of distributed generation (DG), capacitor and OLTC switching along with the placement and sizing of DG.

**Author Contributions:** Conceptualization, J.B.F.I., M.T.R., S.A. and H.M. (Hazlie Mokhlis); methodology, J.B.F.I., M.T.R., T.A. and G.M.S.; software, J.B.F.I., M.T.R., S.A.; validation M.O., T.F.T.M.N.I. and M.T.A.; formal analysis, T.A., H.M. (Hasmaini Mohamad); investigation, S.A., G.M.S. and M.T.A.; resources, H.M. (Hazlie Mokhlis); data curation, T.A.; writing—original draft preparation, J.B.F.I., H.M. (Hazlie Mokhlis), S.A. and T.A.; writing—review and editing, G.M.S., M.O., T.F.T.M.N.I. and

H.M. (Hasmaini Mohamad); supervision, H.M. (Hazlie Mokhlis), M.O. and G.M.S.; project administration, G.M.S; funding acquisition, H.M. (Hazlie Mokhlis). All authors have read and agreed to the published version of the manuscript.

**Funding:** This work was financially supported by the University of Malaya under SATU Joint Research Scheme Program (Grant no. ST014-2020).

**Data Availability Statement:** Not applicable.

**Conflicts of Interest:** The authors declare no conflict of interest.

## Abbreviations

The following abbreviations are used in this manuscript:

AHP	Analytic hierarchy process
BFA	Binary firefly algorithm
CR	Consistency ratio
OLTC	On-load tap changer
PEV	Plug-in electric vehicle
SOC	State of charge
V2G	Vehicle-to-grid
TOU	Time-of-use

## References

- Das, H.S.; Rahman, M.M.; Li, S.; Tan, C.W. Electric vehicles standards, charging infrastructure, and impact on grid integration: A technological review. *Ren. and Sust. Energy Rev.* **2020**, *120*, 109618. [\[CrossRef\]](#)
- Kongjeen, Y.; Bhumkittipich, K. Impact of plug-in electric vehicles integrated into power distribution system based on voltage-dependent power flow analysis. *Energies* **2018**, *11*, 1571. [\[CrossRef\]](#)
- Quirós-Tortós, J.; Ochoa, L.F.; Alnaser, S.W.; Butler, T. Control of EV charging points for thermal and voltage management of LV networks. *IEEE Trans. Power Syst.* **2015**, *31*, 3028–3039. [\[CrossRef\]](#)
- Rahman, M.T.; Abd, Rahim, N.B.; Othman, M.; Mokhlis, H. Plug-in electric vehicle charging coordination considering distribution protection system. In Proceedings of the IEEE PES Asia-Pacific Power and Energy Engineering Conference (APPEEC), Kota Kinabalu, Malaysia, 7–10 October 2018; pp. 51–55. [\[CrossRef\]](#)
- Rahman, M.T.; Othman, M.; Mokhlis, H.; Muhammad, M.A.; Bouchekara, H.R. Optimal fixed charge-rate coordination of plug-in electric vehicle incorporating capacitor and OLTC switching to minimize power loss and voltage deviation. *IEEJ Trans. Electr. Electron. Eng.* **2018**, *13*, 963–970. [\[CrossRef\]](#)
- Suyono, H.; Rahman, M.T.; Mokhlis, H.; Othman, M.; Illias, H.A.; Mohamad, H. Optimal scheduling of plug-in electric vehicle charging including time-of-use tariff to minimize cost and system stress. *Energies* **2019**, *12*, 1500. [\[CrossRef\]](#)
- Sufyan, M.; Rahim, N.A.; Muhammad, M.A.; Tan, C.K.; Raihan, S.R.S.; Bakar, A.H.A. Charge coordination and battery lifecycle analysis of electric vehicles with V2G implementation. *Electr. Power Syst. Res.* **2020**, *184*, 106307. [\[CrossRef\]](#)
- Boonraksa, T.; Marungsri, B. Optimal fast charging station location for public electric transportation in smart power distribution network. In Proceedings of the International Electrical Engineering Congress (iEECON), Krabi, Thailand, 7–9 March 2018; pp. 1–4. [\[CrossRef\]](#)
- Rahman, I.; Mohamad-Saleh, J. Plug-in electric vehicle charging optimization using bio-inspired computational intelligence methods. In *Sustainable Interdependent Networks*; Springer: Cham, Switzerland, 2018; pp. 135–147. [\[CrossRef\]](#)
- Morshed, M.J.; Hmida, J.B.; Fekih, A. A probabilistic multi-objective approach for power flow optimization in hybrid wind-PV-PEV systems. *Appl. Energy* **2018**, *211*, 1136–1149. [\[CrossRef\]](#)
- Mehta, R.; Srinivasan, D.; Khambadkone, A.M.; Yang, J.; Trivedi, A. Smart charging strategies for optimal integration of plug-in electric vehicles within existing distribution system infrastructure. *IEEE Trans. Smart Grid* **2016**, *9*, 299–312. [\[CrossRef\]](#)
- Mehta, R.; Srinivasan, D.; Trivedi, A.; Yang, J. Hybrid planning method based on cost-benefit analysis for smart charging of plug-in electric vehicles in distribution systems. *IEEE Trans. Smart Grid* **2017**, *10*, 523–534. [\[CrossRef\]](#)
- Hajforoosh, S.; Masoum, M.A.; Islam, S.M. Real-time charging coordination of plug-in electric vehicles based on hybrid fuzzy discrete particle swarm optimization. *Electr. Power Syst. Res.* **2015**, *128*, 19–29. [\[CrossRef\]](#)
- Masoum, A.S.; Deilami, S.; Moses, P.S.; Masoum, M.A.; Abu-Siada, A. Smart load management of plug-in electric vehicles in distribution and residential networks with charging stations for peak shaving and loss minimisation considering voltage regulation. *IET Gener. Transm. Distrib.* **2011**, *5*, 877–888. [\[CrossRef\]](#)
- Deilami, S.; Masoum, A.S.; Moses, P.S.; Masoum, M.A. Real-time coordination of plug-in electric vehicle charging in smart grids to minimize power losses and improve voltage profile. *IEEE Trans. Smart Grid* **2011**, *2*, 456–467. [\[CrossRef\]](#)
- Masoum, A.S.; Deilami, S.; Abu-Siada, A.; Masoum, M.A. Fuzzy approach for online coordination of plug-in electric vehicle charging in smart grid. *IEEE Trans. Sustain. Energy* **2014**, *6*, 1112–1121. [\[CrossRef\]](#)

17. Usman, M.; Tareen, W.U.; Amin, A.; Ali, H.; Bari, I.; Sajid, M.; Seyedmahmoudian, M.; Stojcevski, A.; Mahmood, A.; Mekhilef, S. A coordinated charging scheduling of electric vehicles considering optimal charging time for network power loss minimization. *Energies* **2021**, *14*, 5336. [[CrossRef](#)]
18. Cao, C.; Wu, Z.; Chen, B. Electric vehicle–Grid integration with voltage regulation in radial distribution networks. *Energies* **2020**, *13*, 1802. [[CrossRef](#)]
19. Liu, M.; Phanivong, P.K.; Shi, Y.; Callaway, D.S. Decentralized charging control of electric vehicles in residential distribution networks. *IEEE Trans. Control. Syst. Technol.* **2017**, *27*, 266–281. [[CrossRef](#)]
20. Nimalsiri, N.I.; Ratnam, E.L.; Mediwaththe, C.P.; Smith, D.B.; Halgamuge, S.K. Coordinated charging and discharging control of electric vehicles to manage supply voltages in distribution networks: Assessing the customer benefit. *Appl. Energy* **2021**, *291*, 116857. [[CrossRef](#)]
21. Hajforoosh, S.; Masoum, M.A.; Islam, S.M. Online optimal variable charge-rate coordination of plug-in electric vehicles to maximize customer satisfaction and improve grid performance. *Electr. Power Syst. Res.* **2016**, *141*, 407–420. [[CrossRef](#)]
22. Abou, El-Ela, A.A.; El-Sehiemy, R.A.; Kinawy, A.M.; Mouwafi, M.T. Optimal capacitor placement in distribution systems for power loss reduction and voltage profile improvement. *IET Gener. Transm. Distrib.* **2016**, *10*, 1209–1221. [[CrossRef](#)]
23. Arias, N.B.; Franco, J.F.; Lavorato, M.; Romero, R. Metaheuristic optimization algorithms for the optimal coordination of plug-in electric vehicle charging in distribution systems with distributed generation. *Electr. Power Syst. Res.* **2017**, *142*, 351–361. [[CrossRef](#)]
24. Valsera-Naranjo, E.; Martinez-Vicente, D.; Sumper, A.; Villafafila-Robles, R.; Sudria-Andreu, A. Deterministic and probabilistic assessment of the impact of the electrical vehicles on the power grid. In Proceedings of the 2011 IEEE Power and Energy Society General Meeting, Detroit, MI, USA, 24–28 July 2011; pp. 1–8. [[CrossRef](#)]
25. Antúnez, C.S.; Franco, J.F.; Rider, M.J.; Romero, R. A new methodology for the optimal charging coordination of electric vehicles considering vehicle-to-grid technology. *IEEE Trans. Sustain. Energy* **2016**, *7*, 596–607. [[CrossRef](#)]
26. Aghajan-Eshkevari, S.; Azad, S.; Nazari-Heris, M.; Ameli, M.T.; Asadi, S. Charging and discharging of electric vehicles in power systems: An updated and detailed review of methods, control structures, objectives, and optimization methodologies. *Sustainability* **2022**, *14*, 2137. [[CrossRef](#)]
27. Honarmand, M.; Zakariazadeh, A.; Jadid, S. Integrated scheduling of renewable generation and electric vehicles parking lot in a smart microgrid. *Energy Convers. Manag.* **2014**, *86*, 745–755. [[CrossRef](#)]
28. Jian, L.; Zheng, Y.; Xiao, X.; Chan, C.C. Optimal scheduling for vehicle-to-grid operation with stochastic connection of plug-in electric vehicles to smart grid. *Appl. Energy* **2015**, *146*, 150–161. [[CrossRef](#)]
29. Fu, H.; Han, Y.; Wang, J.; Zhao, Q. A novel optimization of plug-in electric vehicles charging and discharging behaviors in electrical distribution grid. *J. Electr. Comput. Eng.*, **2018**, *2018*, 5091084. [[CrossRef](#)]
30. Reddy, K.R.; Meikandasivam, S.; Vijayakumar, D. A novel strategy for maximization of plug-In electric vehicle’s storage utilization for grid support with consideration of customer flexibility. *Electr. Power Syst. Res.* **2019**, *170*, 158–175. [[CrossRef](#)]
31. Nimalsiri, N.I.; Ratnam, E.L.; Smith, D.B.; Mediwaththe, C.P.; Halgamuge, S.K. Coordinated charge and discharge scheduling of electric vehicles for load curve shaping. *IEEE Trans. Intell. Transp. Syst.* **2021**, *13*, 7653–7665. [[CrossRef](#)]
32. Jozi, F.; Mazlumi, K.; Hosseini, H. December. Charging and discharging coordination of electric vehicles in a parking lot considering the limitation of power exchange with the distribution system. In Proceedings of the IEEE 4th International Conference on Knowledge-Based Engineering and Innovation (KBEI), Tehran, Iran, 22 December 2017; pp. 0937–0941. [[CrossRef](#)]
33. Yang, X.S. *Nature-Inspired Metaheuristic Algorithms*; Luniver Press: Beckington, UK, 2008; pp. 242–246.
34. Palit, S.; Sinha, S.N.; Molla, M.A.; Khanra, A.; Kule, M. A cryptanalytic attack on the knapsack cryptosystem using binary firefly algorithm. In Proceedings of the 2nd International Conference on Computer and Communication Technology, Allahabad, India, 15–17 September 2011; pp. 428–432. [[CrossRef](#)]
35. Saaty, T.L. Decision making for leaders. *IEEE Trans. Syst. Man Cybern.* **1985**, *3*, 450–452. [[CrossRef](#)]
36. Ali, T.; Nahian, A.J.; Ma, H. A hybrid multi-criteria decision-making approach to solve renewable energy technology selection problem for Rohingya refugees in Bangladesh. *J. Clean. Prod.* **2020**, *273*, 122967. [[CrossRef](#)]
37. Kim, D.M.; Kim, J.O. Design of emergency demand response program using analytic hierarchy process. *IEEE Trans. Smart Grid* **2012**, *3*, 635–644. [[CrossRef](#)]
38. Mu, E.; Pereyra-Rojas, M. Understanding the analytic hierarchy process. In *Practical Decision Making*; Springer: Cham, Switzerland, 2017; pp. 7–22. [[CrossRef](#)]

**Disclaimer/Publisher’s Note:** The statements, opinions and data contained in all publications are solely those of the individual author(s) and contributor(s) and not of MDPI and/or the editor(s). MDPI and/or the editor(s) disclaim responsibility for any injury to people or property resulting from any ideas, methods, instructions or products referred to in the content.